

# Intense Visible Photoluminescence from $C_{46}H_{22}N_8O_4KM$ (M = Co, Fe, Pb) Derivatives Thin Films

María Elena Sánchez<sup>1</sup>, Juan Carlos Alonso<sup>2</sup>, Jerry Nathan Reider<sup>1</sup>

<sup>1</sup>Faculty of Engineering, Anáhuac México Norte University, Avenida Universidad Anáhuac 46,  
Col. Lomas Anáhuac, Huixquilucan, Estado de México, México

<sup>2</sup>Materials Research Institute, National Autonomous University of México (UNAM),  
Coyoacán, México

E-mail: [elena.sanchez@anahuac.mx](mailto:elena.sanchez@anahuac.mx)

Received August 3, 2011; revised September 27, 2011; accepted October 7, 2011

## Abstract

Strong visible photoluminescence (PL) at room temperature is obtained from thermal-evaporated thin solid films of Metallophthalocyanine (M = Co, Fe, Pb) and double potassium salt from 1,8 dihydroxyanthraquinone. The PL of all the investigated samples is observed with the naked eye in a bright background. The deconvolution of the normalized PL spectra shows that each PL spectrum is composed of four emission bands which peak at approximately the same energies of 2.1, 2.2 and 2.4 eV and whose intensities and widths depend upon the structure of the complexes. FTIR and ellipsometry are employed to investigate the structural differences among the films. The optical absorption of the films is also investigated to evaluate the changes in the electronic structure of these metal organic compounds, with respect to other metallophthalocyanines thin films. Our results suggest that the visible PL comes from radiative transitions between energy levels associated to the double potassium salt coordination to the metallic ion in the phthalocyanine.

**Keywords:** Thin Films, Optical Properties, Photoluminescence

## 1. Introduction

Since the report, more than two decades ago, of efficient electroluminescence (EL) from organic thin films [1], the use of small organic molecules and organic polymers in the fabrication of organic light emitting diodes (OLED's) attracts considerable interest for solid state displays and lighting applications [3]. A typical OLED comprises a luminescent organic thin film sandwiched in-between an electron transport layer and a hole transport layer bound by two electrodes. One of the foremost class of planar organic molecular semiconductors, used as electron or hole transport layer, is that of the metallophthalocyanines (MPcs). Optical properties of these materials, among them the luminescence, are strongly related to the valence band electronic configuration, as well as the excitation and the de-excitation processes between highest occupied molecular orbitals (HOMO) and lowest unoccupied molecular orbitals (LUMO) [4]. The optical properties of MPcs are very important for understanding their molecular structure and improving the performance of devices made with phthalocyanines.

In thin films, MPcs usually present a given crystalline form or may be amorphous depending mainly upon the molecular self-stacking ability of the derivate, but also upon the thin film fabrication procedure [5]. Moreover, the control of film structure is of great importance in thin film technology since the opto-electronic properties such as the photogeneration of charge carriers, highly depends on the degree of molecular organization [5]. In thin films, molecules crystallize and their interaction is significant, so that dramatic changes occur in their optical properties, making them much more complicated [6]. Since these organic materials in the solid film form are applied in the production of the majority of modern optoelectronic devices, the knowledge of their excited electronic states and relaxation processes is particularly important [6]. Photoluminescence (PL) properties in the solid (or crystalline) phases have been investigated for only a few MPcs materials such as H2Pc, ZnPc, AlClPc, VOPc, TiOPc, MgPc and AlBrPc [7]. PL is a powerful probe for assessing the excited states, because useful information can be obtained by measuring its properties such as quantum yields, spectra, time decay, and temperature

dependence [7]. For the electroluminescence (EL) application, PL properties provide important reference data, because the EL spectra and the EL emission efficiencies of the materials can be estimated through the corresponding PL spectra and the quantum yields. Therefore, it is important to investigate PL phenomena of MPC compounds in the solid phases, whereas the luminescence of most of these organic compounds lies in the red and near-infrared regions and with low efficiency at room temperature [8-10]. Studies on the optical properties of phthalocyanine-derived thin films show that the optical absorption and luminescence of these new organic compounds with complex structures can be tailored and/or modified to decrease or increase the near-IR luminescence efficiency [11-14], and even produce polarized red luminescence [15] or strong blue photoluminescence [16]. In this paper, we report intense photoluminescence from MPCs-derived thin films prepared by vacuum thermal evaporation of semiconductor powders from iron, lead and cobalt phthalocyanines with a double potassium salt derived from 1,8 dihydroxyanthraquinone ( $K_2C_{14}H_6O_4$ ). Vibrational spectra are obtained and the refractive indices and absorption coefficients are determined for the studied samples.

## 2. Experimental Details

The raw materials used in this work are obtained from commercial sources with no purification prior to their use. The powders of the three compounds;  $C_{46}H_{22}N_8O_4KFe$ ,  $C_{46}H_{22}N_8O_4KPb$  and  $C_{46}H_{22}N_8O_4KCo$ , are synthesized from metallic phthalocyanines and double potassium salt derived from 1,8 dihydroxyanthraquinone, using the procedure reported previously [17]. Thin film deposition of these compounds is carried out by vacuum thermal evaporation onto Corning 7059 glass slices and (100) single-crystalline silicon (c-Si), 200  $\Omega$ -cm wafers. The substrate temperatures are kept at 298 K during deposition. The Corning 7059 substrates are ultrasonically degreased in warm ethanol and dried in a nitrogen atmosphere. The silicon substrates are chemically etched with a p-etch solution (10 ml HF, 15 ml  $HNO_3$ , and 300 ml  $H_2O$ ) in order to remove the native oxide from the c-Si surface. The evaporation source is a molybdenum boat with two grids. The temperature through the molybdenum boat is slowly increased to 453 K, below the first significant signal change observed in the thermo-gravimetric analysis thermogram, in order to prevent thermal decomposition of the compound and to identify the phase changes (evaporation, sublimation). All samples are obtained using the same deposition system, with the crucible and substrates arranged in the same geometry. The base pressure in the deposition chamber before thin film

deposition and the amount of mass inside the crucible are the same in all cases. In spite of these similarities, significant differences in the thickness of deposited films are detected, which may be related to differences in the sublimation processes for the compounds used. An atomic force microscope (AFM) coupled to a potentiostat/galvanostat module from Digital Instruments is also used to investigate the morphology of the thin films. A Gaertner L117 Ellipsometer equipped with a He-Ne laser ( $\lambda = 632.8$  nm) is used to measure the thickness and refractive index of the films. The thickness of the films is also measured by means of a Sloan Dektak IIA profilometer. The chemical bonding behavior is analysed by means of a Fourier transform infrared (FTIR) spectrophotometer (Nicolet-210). Photoluminescence (PL) measurements are carried out in a dark room at room temperature, using a beam ( $\lambda = 325$  nm, 25 mW) from a Kimmon He-Cd laser as excitation source, with an incident angle of  $45^\circ$  relative to the normal of the sample. The luminescence is collected at an angle normal to the sample using a quartz optic fiber and measured in the range from 350 nm to 800 nm with a Fluoromax-Spex spectrofluorometer. Ultraviolet-visible (UV-Vis) transmission measurements are carried out in the range from 300 to 1100 nm using a double-beam PerkinElmer Lambda 35 UV-Vis spectrophotometer. For PL, infrared and ellipsometric measurements the substrates used are (100) oriented c-Si slices with 200  $\Omega$ -cm resistivity. For AFM and optical transmission measurements, the substrates are naked 7059 Corning glass slices. The electric conductivity at 298 K of the films is studied by means of a four-point probe; for these measurements, the substrates are Corning 7059 glass slices coated with four metallic strips acting as electrodes. The strips are deposited by thermal evaporation. In order to get an ohmic contact with the deposited films, the electrodes are made from silver.

## 3. Results and Discussion

The purpose of IR spectroscopy on thin films is determining if there were significant chemical changes on the MPCs-derived compounds during the thermal evaporation used to prepare the films. However, chemical changes or reactions are not expected to occur owing to the thermal stability present in these compounds. **Table 1** shows the characteristic bands for these compounds on thin film. These results appear to indicate that the deposited compound is not affected by the thermal evaporation and deposition processes during film growth. The deposited films are formed by the same macro-ions as those of the original synthesized powder, as indicated by comparison between the location of the absorption bands in

**Table 1. Characteristic FT-IR bands for powders and thin films (cm<sup>-1</sup>).**

| COMPOUND   | $\nu$ (C-H) (cm <sup>-1</sup> ) | $\nu$ (C-C) (cm <sup>-1</sup> ) | $\nu$ (C-N) (cm <sup>-1</sup> ) | $\nu$ (C = O) (cm <sup>-1</sup> ) | $\nu$ (C-O) (cm <sup>-1</sup> ) |
|--|---------------------------------|---------------------------------|---------------------------------|-----------------------------------|---------------------------------|
| C <sub>46</sub> H <sub>22</sub> N <sub>8</sub> O <sub>4</sub> KFe Thin Film  | 3049, 2851                      | 1610, 630                       | 1284, 1157, 1070                | 1606                              | 1089                            |
| C <sub>46</sub> H <sub>22</sub> N <sub>8</sub> O <sub>4</sub> KFe KBr pellet | 3048, 2855                      | 1607, 632                       | 1285, 1158, 1070                | 1604                              | 1091                            |
| C <sub>46</sub> H <sub>22</sub> N <sub>8</sub> O <sub>4</sub> KPb Thin Film  | 3048, 2851                      | 1603, 623                       | 1277, 1156, 1077                | 1602                              | 1087                            |
| C <sub>46</sub> H <sub>22</sub> N <sub>8</sub> O <sub>4</sub> KPb KBr pellet | 3050, 2853                      | 1608, 626                       | 1274, 1159, 1079                | 1602                              | 1088                            |
| C <sub>46</sub> H <sub>22</sub> N <sub>8</sub> O <sub>4</sub> KCo Thin Film  | 3045, 2852                      | 1605, 625                       | 1287, 1161, 1071                | 1609                              | 1085                            |
| C <sub>46</sub> H <sub>22</sub> N <sub>8</sub> O <sub>4</sub> KCo KBr pellet | 3044, 2849                      | 1608, 628                       | 1284, 1164, 1070                | 1610                              | 1083                            |

the spectra of the synthesized powders, and those of the deposited films [17]. When compounds have the film form, the signs show slight changes in their location because, in all thin films deposited by any method, there are inner stresses that affect the angles and energies of intramolecular bonds. **Table 1** shows the signs corresponding to macrocycle [18,19]: two bands appearing at about 3048 and 2854 cm<sup>-1</sup> are assigned as CH (symmetric stretching vibrations in the ring and asymmetric stretching vibrations as alkyl). The band appearing at 1609 cm<sup>-1</sup> is assigned to the C-C stretching vibration in pyrrole. Additionally, the band appearing at 625 cm<sup>-1</sup> is assigned the C-C macrocycle ring deformation. The bands appearing at 1284, 1161 and 1070 are assigned to the C-N in isoindole in plane band in pyrrole stretching vibration, respectively. The spectral pattern in this region depends strongly upon the molecular structure of the complexes and its chemical structure for the central metal with D<sub>4h</sub> molecular symmetry [19]. It may be noticed [17] that the materials from the MPC and double potassium salt derived from 1,8-dihydroxyanthraquinone exhibit C = O and C-O functional groups with wavelengths 1600 cm<sup>-1</sup> and 1080 cm<sup>-1</sup>, respectively [17-20]. Due to the bond of phthalocyanine to the potassium double salt anion (C<sub>14</sub>H<sub>6</sub>O<sub>4</sub>)<sup>2-</sup>, a characteristic band around 1662 cm<sup>-1</sup> assigned to the elongation vibration of carbonile group C = O in the quinones is observed. In addition, the band near 1083 cm<sup>-1</sup> corresponding to the C-O elongation vibration is present, as well [17-20].

In order to obtain information about the quality of the films we investigate the surface morphology by AFM. The AFM analysis of the evaporated films displays a homogeneous distribution of small spherical aggregates. The RMS roughness values are shown in **Table 2**. The refractive indices ( $n$ ) of the films, obtained from ellipsometric measurements are shown in **Table 2**, as well as the reflectance percentages at normal incidence, calculated using the equation:

$$R = 100(n-1)^2 / (n+1)^2 \quad (1)$$

The refraction index, as well as the reflectance, de-

pend upon the thickness of the thin film: the lead-based film is the one which shows the least thickness, associated with higher values for both the reflectance and refraction indexes. It is noticed that at thin thicknesses all films become transparent and no light is scattered or absorbed. The electrical conductivity of each material is evaluated at 25°C. These results are shown in **Table 2** with the C<sub>46</sub>H<sub>22</sub>N<sub>8</sub>O<sub>4</sub>KCo material presenting the highest conductivity. Generally, the conductivity at room temperature decreases when increasing the atomic number of the central metal except Fe. This may be due to the change of chemical structure of Fe and it takes place for Fe<sup>2+</sup> and Fe<sup>3+</sup> [19]. Besides, electrical conductivity values at room temperature for all materials are in the electrical conductivity range for semiconducting molecular materials (10<sup>-6</sup> to 10<sup>1</sup> S·cm<sup>-1</sup>) [17]. This is important since a molecular semiconductor is generally defined in terms of its conductivity at room temperature and its behavior with temperature. Conductivity is also related to impurity types, location and concentration, structure, stacking and overlaps between orbitals. The charge transfer in these compounds, occurs via phthalocyanine rings that stacks, generating a direct  $\pi$  -  $\pi$  interaction between adjacent molecules in the pile, but very weak interactions between molecules in adjacent piles. The electric charges transport on them is due to the highly ordered structure that form; apparently there is a marked anisotropy as a consequence of the stacking of phthalocyanine columns in columnar piles, along which the electric charges flow.

**Figure 1(a)** shows the photoluminescence (PL) spectra of the films, obtained at room temperature (300 K). It is evident from **Figure 1(a)** that these films exhibit luminescence in the visible region. These results are important since most of the reports and studies on the luminescence of this type of metal organic compounds are made in the IR region. The PL spectra of the three samples show two main central peaks and two side shoulders located at similar wavelengths but with different intensities. The absorbance (A) spectra of the films (**Figure 1(b)**) show more complicated structure with optical ab-

**Table 2. AFM evaluation of the thin film roughness, film thickness, refraction index, reflectance and electrical conductivity results for thin films.**

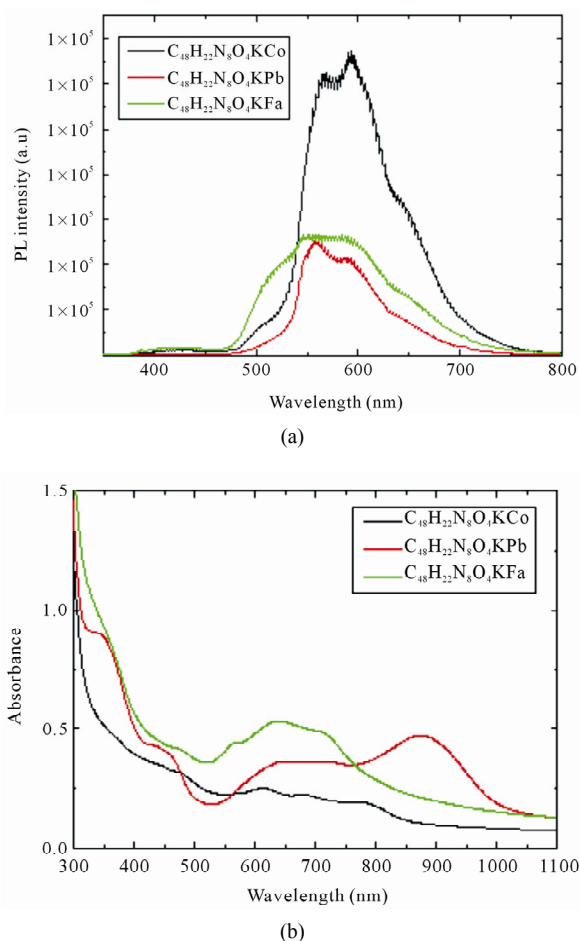
| Optical and Electrical parameters       | C <sub>46</sub> H <sub>22</sub> N <sub>8</sub> O <sub>4</sub> KFe | C <sub>46</sub> H <sub>22</sub> N <sub>8</sub> O <sub>4</sub> KPb | C <sub>46</sub> H <sub>22</sub> N <sub>8</sub> O <sub>4</sub> KCo |
|---|---|---|---|
| RMS roughness (nm)                      | 84.79   | 74.37   | 89.54   |
| Film thickness (nm)                     | 133   | 108   | 170   |
| Refraction index                        | 2.6   | 2.9   | 2.1   |
| % Reflectance                           | 19  | 24  | 12  |
| Electrical conductivity at 298 K (S/cm) | 1.57E-5   | 1.36E-5   | 4.96E-5   |

sorption peaks and edges distributed in the wavelength range from infrared to ultraviolet. It is well known that the absorption spectrum for phthalocyanines originates from molecular orbitals within the aromatic  $18\pi$  electron system and from overlapping orbitals on the central metal atom [18]. The compounds C<sub>46</sub>H<sub>22</sub>N<sub>8</sub>O<sub>4</sub>KPb and C<sub>46</sub>H<sub>22</sub>N<sub>8</sub>O<sub>4</sub>KFe exhibit a similar behavior in the visible region in comparison with C<sub>46</sub>H<sub>22</sub>N<sub>8</sub>O<sub>4</sub>KCo. This, in turn, can be explained by the different electronic configuration of the central metallic ion and the number of electrons in the outer level:  $3d^6$  for C<sub>46</sub>H<sub>22</sub>N<sub>8</sub>O<sub>4</sub>KFe,  $6S^2$  for C<sub>46</sub>H<sub>22</sub>N<sub>8</sub>O<sub>4</sub>KPb and  $3d^7$  for C<sub>46</sub>H<sub>22</sub>N<sub>8</sub>O<sub>4</sub>KCo [19].

In order to investigate the origin of the visible photoluminescence and the relationship with the optical absorption and electronic structure of these thin films, the PL and absorbance spectra of **Figure 1** were plotted together in an overlapping scheme in terms of photon energy. These plots are presented in **Figure 2**. Since the analyzed samples have different thicknesses (see **Table 2**) and the PL intensity depends upon this parameter, the PL spectra of **Figure 2** are normalized relative to the maximum intensity in order to neglect this dependence. As can be seen from these plots, there is strong absorbance for the three samples at the energy of the excitation source photons (marked with an arrow). This means that the photons from the excitation source are efficiently absorbed by the samples, which partly explains their efficient PL. It is interesting to note that the start and end energies (also marked with arrows in the spectra) of the main photoluminescence band correspond to energies where optical absorption bands or edges lie. These energies are similar for the three samples.

A close examination of the absorption band in the UV region, which is known as the Soret band or the B-band (3 - 4.5 eV) [21], reveals one peak around 3.8 eV for C<sub>46</sub>H<sub>22</sub>N<sub>8</sub>O<sub>4</sub>KFe, C<sub>46</sub>H<sub>22</sub>N<sub>8</sub>O<sub>4</sub>KPb and C<sub>46</sub>H<sub>22</sub>N<sub>8</sub>O<sub>4</sub>KCo (see **Figure 2** and **Table 3**). This strongly indicates the presence of a d-band associated with the central metal atom. This is because PcM(L) has partially occupied d bands. The absorption band near 4.0 eV may be due to  $\pi$ -d transition. The other well-known band of the phthalocyanine molecule, namely Q-band, appears in the region

between 1.4 and 2.6 eV. The Q-band is split into two distinct peaks in the visible region due to molecule aggregation or molecular distortion [21]. As observed from **Figure 2**, the distinct characterized peaks for thin films in the visible region have been generally been interpreted in terms of  $\pi$  -  $\pi^*$  excitation between bounding and anti-bounding molecular orbitals [21]. The Q-band consists of a high-energy peak around 2.6 eV and a low energy

**Figure 1. (a) Photoluminescence and (b) Absorbance spectra of C<sub>46</sub>H<sub>22</sub>N<sub>8</sub>O<sub>4</sub>KCo, C<sub>46</sub>H<sub>22</sub>N<sub>8</sub>O<sub>4</sub>KPb, C<sub>46</sub>H<sub>22</sub>N<sub>8</sub>O<sub>4</sub>KFe, thin films.**

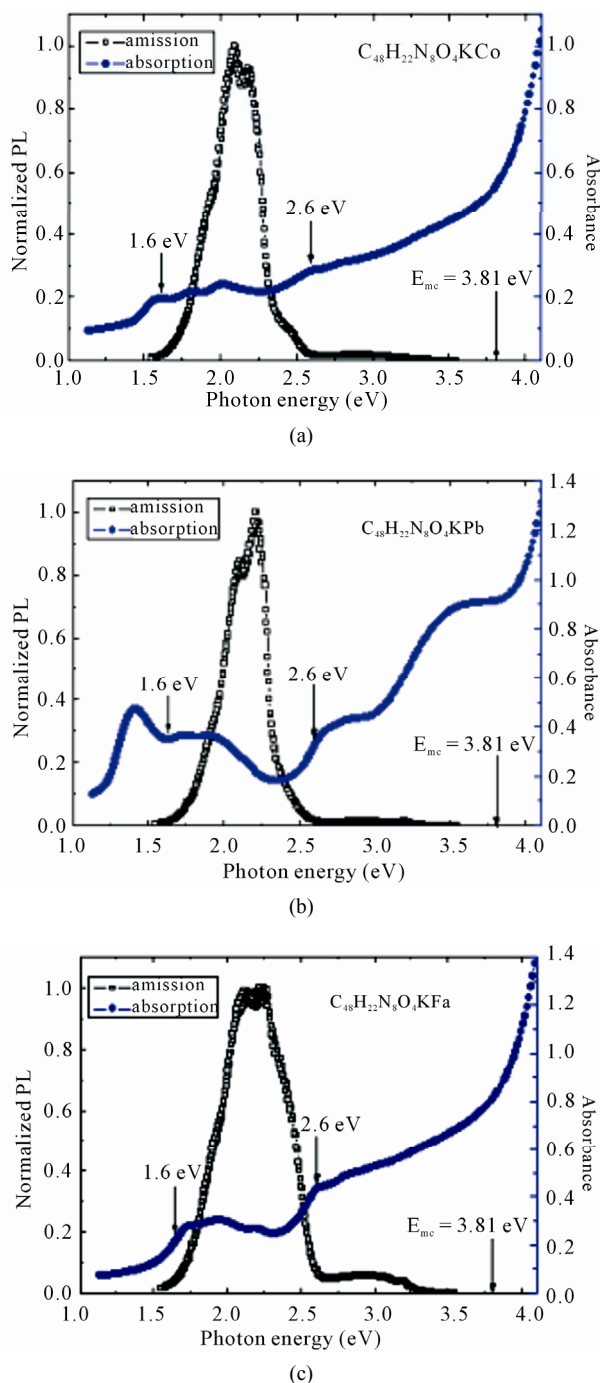


**Figure 2.** Normalized PL and absorbance versus photon energy of (a)  $C_{46}H_{22}N_8O_4KCo$ , (b)  $C_{46}H_{22}N_8O_4KPb$ , (c)  $C_{46}H_{22}N_8O_4KFe$ , thin films.

shoulder at 1.6 eV. The high-energy peak of the Q band is assigned to the first  $\pi - \pi^*$  transition on the phthalocyanine macrocycle. The low-energy peak of the Q band is explained either, as a second  $\pi - \pi^*$  transition, as an excitation peak, as a vibrational internal interval and as a surface state [21]. The Q-band is associated to the dou-

ble potassium salt coordination to the metallic ion in the phthalocyanine. The presence of this absorption band may be interpreted as an overlapping of  $\pi$  orbitals through the bidentate ligand. The conjugated double bonds within the structure of the films create electron orbitals overlapping between the molecules ( $\pi$  orbitals). Electrons are therefore able to transfer energy throughout the structure and become responsible for the absorption spectra [21]. The normalized PL spectra are deconvoluted with four Gaussian functions, as shown in **Figure 3**. As can be seen, the four Gaussian functions peak at approximately the same energies of 2.1 eV (orange), 2.2 eV (yellow) and 2.3 eV (green), whose intensities and widths depend upon the specific metal in the complexes organic structure. **Table 3** summarizes the energy positions of all the absorption peaks and luminescent peaks of the samples. Although the curves are maximum emission peaks, close together in their energy value, it shows greater luminescence for the lead-based compound. This was due to the location of the electrons in the final energy level of  $Pb^{2+}$  in the macrocycle. The compounds of  $Fe^{2+}$  and  $Co^{2+}$  have similar values for the area beneath the curve, taking into account the available 3d electrons.

According to our data, the PL in phthalocyanine thin films is substantially affected by the intramolecular structure. The different metallic ions in the phthalocyanine produce differences in the PL peak in the visible range [22]. The incorporation of metallic ions in the phthalocyanine molecule ( $Fe^{2+}$ ,  $Co^{2+}$ ,  $Pb^{2+}$ ) may affect the intensity and width of the peak, but it does not significantly change the general structure of the molecule. In this case, the divalent cation  $Pb^{2+}$  exhibits the largest absorption peaks energy, probably due to the fact that the outermost orbital in this cation is completed and reflects the electrostatic nature of the coordination process in these films. Nevertheless, the PL peaks obtained in these materials are higher than the pure analog metallic complexes [14,15], suggesting that the addition of the double potassium salt from 1,8 dihydroxyanthraquinone improves the photoluminescence (PL) at room temperature. It is possible that the ligand increase in the anisotropy arises from a columnar disposition of the phthalocyanines-ligand.

## 4. Conclusions

Thin films of iron, lead and cobalt phthalocyanines and double potassium salt derived from 1,8-dihydroxyanthraquinone are deposited by vacuum thermal evaporation. According to the IR spectra, they are formed by the same chemical units as those of the corresponding synthesized powders. The conductivity results for materials  $C_{46}H_{22}N_8O_4KFe$ ,  $C_{46}H_{22}N_8O_4KPb$  and  $C_{46}H_{22}N_8O_4KCo$

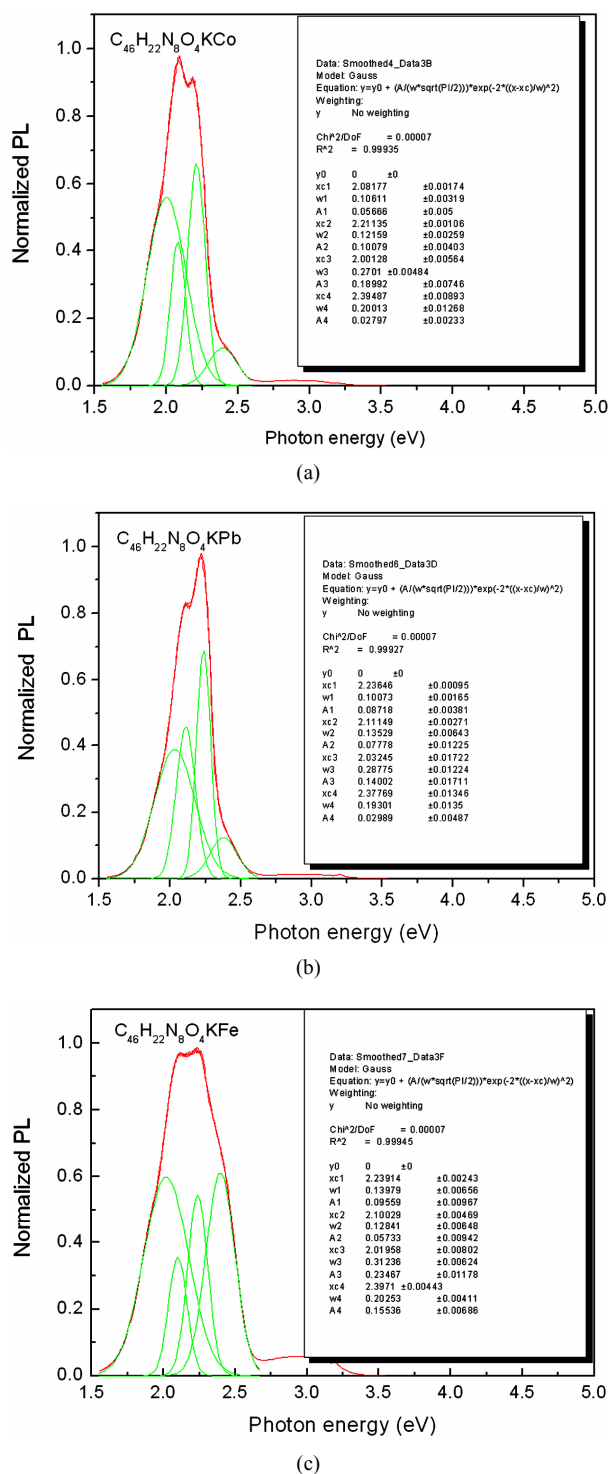


**Figure 3. Gaussian fitting of the normalized PL spectra of (a)  $C_{46}H_{22}N_8O_4KCo$ , (b)  $C_{46}H_{22}N_8O_4KPb$ , (c)  $C_{46}H_{22}N_8O_4KFe$ , thin films.**

are  $1.57 \times 10^{-5} \text{ S}\cdot\text{cm}^{-1}$ ,  $1.36 \times 10^{-5} \text{ S}\cdot\text{cm}^{-1}$  and  $4.96 \times 10^{-5} \text{ S}\cdot\text{cm}^{-1}$ . All the investigated thin films exhibit strong emission in the visible region. Our results suggest that

**Table 3. Absorption and emission energies of the thin films.**

| Sample                  | Absorption peaks energy (eV)  | Emission peaks energy (eV) | PL intensity. Area under curve (A.U.) <sup>2</sup> |
|-------------------------|-------------------------------|----------------------------|--|
| $C_{46}H_{22}N_8O_4KPb$ | 1.4, 1.7, 1.91, 2.6, 3.5, 3.8 | 2.2, 2.1                   | $6.04 \times 10^5$                                 |
| $C_{46}H_{22}N_8O_4KCo$ | 1.6, 1.8, 2.0, 2.6, 3.4, 3.8  | 2.3, 2.1                   | $2.7 \times 10^5$                                  |
| $C_{46}H_{22}N_8O_4KFe$ | 1.7, 1.9, 2.2, 2.6, 3.8       | 2.3, 2.1                   | $3.9 \times 10^5$                                  |

the visible PL in these complex molecules is originated by the split and broadening of the Q and Soret bands of the phthalocyanines, which generate energy levels where radiative transitions can occur. The PL and absorption spectra in the investigated compounds is strongly influenced by their molecular structures and the nature of metallic ion has smaller influence on the transition energies of the Q and Soret bands. These organic thin films can be used as electroluminescent materials in OLEDs and this application is subject for further studies.

## 5. Acknowledgements

The authors wish to acknowledge Juan Manuel Garcia León and Arturo Rodriguez for his technical assistance.

## 6. References

- [1] C. W. Tang and S. A. VanSlyke, "Organic Electroluminescent Diodes," *Applied Physics Letters*, Vol. 51, No. 12, 1987, pp. 913-915.
- [2] T. Hu and J. P. Desai, "Soft-Tissue Material Properties under Large Deformation: Strain Rate Effect," *Proceedings of the 26th Annual International Conference of the IEEE EMBS*, San Francisco, 1-5 September 2004, pp. 2758-2761.
- [3] T. K. Hatwar and J. Spindler, "Development of White OLED Technology for Application in Full-Color Displays and Solid-State Lighting in Luminescent Materials and Applications," In: A. Kitai, Ed., *Luminescent Materials and Applications*, John Wiley & Sons Ltd., West Sussex, pp. 111-159.
- [4] N. Peltekis, B. N. Holland, S. Krishnamurthy, I. T. McGovern, N. R. J. Poolton, S. Patel and C. McGuinness, "Electronic and Optical Properties of Magnesium Phthalocyanine (MgPc) Solid Films Studied by Soft X-Ray Excited Optical Luminescence and X-Ray Absorption Spectroscopies," *Journal of the American Chemical Society*, Vol. 130, No. 39, 2008, pp. 13008-13012. doi:10.1021/ja803063b
- [5] T. Del Caño, V. Parra, M. L. Rodríguez Méndez, R. F. Aroca and J. A. De Saja, "Characterization of Evaporated trivalent and Tetravalent Phthalocyanines Thin Films: Different Degree of Organization," *Applied Surface Sci-*



- ence, Vol. 246, No. 4, 2005, pp. 327-333. [doi:10.1016/j.apsusc.2004.11.036](https://doi.org/10.1016/j.apsusc.2004.11.036)
- [6] M. Wojdyła, W. Bala, B. Derkowska, M. Rebarz and A. Korcala, "The Temperature Dependence of Photoluminescence and Absorption Spectra of Vacuum-Sublimed Magnesium Phthalocyanine Thin Films," *Optical Materials*, Vol. 30, No. 5, 2008, pp. 734-739. [doi:10.1016/j.optmat.2007.02.023](https://doi.org/10.1016/j.optmat.2007.02.023)
- [7] Y. Sakakibara, R. N. Bera, T. Mizutani, K. Ishida, M. Tokumoto and T. Tani, "Photoluminescence Properties of Magnesium, Chloroaluminum, Bromoaluminum, and Metal-Free Phthalocyanine Solid Films," *Journal of Physical Chemistry B*, Vol. 105, No. 8, 2001, pp. 1547-1553. [doi:10.1021/jp002943o](https://doi.org/10.1021/jp002943o)
- [8] J. H. Sharp and M. Lardon, "Spectroscopic Characterization of a New Polymorph of Metal-Free Phthalocyanine," *Journal of Physical Chemistry*, Vol. 72, No. 9, pp. 3230-3235.
- [9] K. Yoshino, M. Hikida and K. Tatsuno, "Emission Spectra of Phthalocyanine Crystals," *Journal of the Physical Society of Japan*, Vol. 34, No. 2, 1973, pp. 441-445. [doi:10.1143/JPSJ.34.441](https://doi.org/10.1143/JPSJ.34.441)
- [10] M. S. Liao and S. Scheiner, "Electronic Structure and Bonding in Metal Phthalocyanines, Metal = Fe, Co, Ni, Cu, Zn, Mg," *The Journal of Chemical Physics*, Vol. 114, No. 22, 2001, pp. 9780-9791. [doi:10.1063/1.1367374](https://doi.org/10.1063/1.1367374)
- [11] B. Blanzat, C. Barthou and N. Tercier, "Energy Transfer in Solid Phases of Octasubstituted Phthalocyanine Derivatives," *Journal of the American Chemical Society*, Vol. 109, No. 24, 1987, pp. 6193-6194. [doi:10.1021/ja00254a054](https://doi.org/10.1021/ja00254a054)
- [12] W. H. Flora, H. K. Hall and N. R. Armstrong, "Guest Emission Processes in Doped Organic Light-Emitting Diodes: Use of Phthalocyanine and Naphthalocyanine Near-IR Dopants," *Journal of Physical Chemistry B*, Vol. 107, No. 5, 2003, pp. 1142-1150. [doi:10.1021/jp021368g](https://doi.org/10.1021/jp021368g)
- [13] T. Del Caño, J. A. Sajab and R. Aroca, "Emission Enhancement in Chlorogallium Phthalocyanine-N, N9-Bis (Neopentyl)-3,4,9,10-Perylenebis(Dicarboximide) Mixed Films," *Thin Solid Films*, Vol. 425, No. 1-2, 2003, pp. 292-296. [doi:10.1016/S0040-6090\(02\)01107-0](https://doi.org/10.1016/S0040-6090(02)01107-0)
- [14] W. Freyer, C. Neacsu and M. Raschke, "Absorption, Luminescence, and Raman Spectroscopic Properties of Thin Films of Benzo-Annulated Metal-Free Porphyrazines," *Journal of Luminescence*, Vol. 128, No. 4, 2008, pp. 661-672. [doi:10.1016/j.jlumin.2007.11.070](https://doi.org/10.1016/j.jlumin.2007.11.070)
- [15] D. Yan, S. Qin, L. Chen, J. Lu, J. Ma, M. Wei, D. G. Evans and X. Duan, "Thin Film of Sulfonated Zinc Phthalocyanine/Layered Double Hydroxide for Achieving Multiple Quantum Well Structure and Polarized Luminescence," *Chemical Communications*, Vol. 46, No. 45, 2010, pp. 8654-8656. [doi:10.1039/c0cc02129f](https://doi.org/10.1039/c0cc02129f)
- [16] Y. Zhang, X. Sun, Y. Niu, R. Xu, G. Wang and Z. Jian, "Synthesis and Characterization of Novel Poly(Aryl Ether ketone)s with Metallophthalocyanine Pendant Unit from a New Bisphenol Containing Dicyanophenyl Side Group," *Polymer*, Vol. 47, No. 5, 2006, pp. 1569-1574. [doi:10.1016/j.polymer.2005.12.068](https://doi.org/10.1016/j.polymer.2005.12.068)
- [17] M. E. Sánchez-Vergara, M. A. Ruiz Farfán, J. R. Álvarez, A. Ponce Pedraza, A. Ortiz and C. Álvarez-Toledano, "Electrical and Optical Properties of C<sub>46</sub>H<sub>22</sub>N<sub>8</sub>O<sub>4</sub>KM (M=Co, Fe, Pb) Molecular-Material Thin Films Prepared by the Vacuum Thermal Evaporation Technique," *Spectrochimica Acta Part A: Molecular and Biomolecular Spectroscopy*, Vol. 66, No. 3, 2007, pp. 561-567. [doi:10.1016/j.saa.2006.03.040](https://doi.org/10.1016/j.saa.2006.03.040)
- [18] G. Socrates, "Infrared and Raman Characteristic Group Frequencies: Tables and Charts," 3rd Edition, John Wiley and Sons, Hoboken, 2001.
- [19] R. Seoudi, G. S. El-Bahy and Z. A. El Sayed, "FTIR, TGA and DC Electrical Conductivity Studies of Phthalocyanine and Its Complexes," *Journal of Molecular Structure*, Vol. 753, No. 1-3, 2005, pp. 119-126. [doi:10.1016/j.molstruc.2005.06.003](https://doi.org/10.1016/j.molstruc.2005.06.003)
- [20] M. E. Sánchez Vergara, A. Ortiz Rebollo, J. R. Alvarez and M. Rivera, "Molecular Materials Derived from MPC (M = Fe, Pb, Co) and 1,8-Dihydroxiantraquinone Thin Films: Formation, Electrical and Optical Properties," *Journal of Physics and Chemistry of Solids*, Vol. 69, No. 1, 2008, pp. 1-7. [doi:10.1016/j.jpcs.2007.07.084](https://doi.org/10.1016/j.jpcs.2007.07.084)
- [21] M. M. El-Nahass, A. M. Farag, K. F. Abd El-Rahman and A. A. A. Darwish, "Dispersion Studies and Electronic Transitions in Nickel Phthalocyanine Thin Films," *Optics & Laser Technology*, Vol. 37, No. 7, 2005, pp. 513-523. [doi:10.1016/j.optlastec.2004.08.016](https://doi.org/10.1016/j.optlastec.2004.08.016)
- [22] G. A. Kumar, J. Thomas, N. George, B. A. Kumar, P. Radhakrishnan, V. P. N. Nampoore and C. P. G. Vallabhan, "Optical Absorption Studies of Free (H<sub>2</sub>Pc) and Rare Earth (RePc) Phthalocyanine Doped Borate Glasses," *Physics and Chemistry of Glasses*, Vol. 41, No. 2, 2000, pp. 89-93.